Molecular Biology of the Cell
Vol. 11, 2057–2068, June 2000

Dynamic Regulation of Activated Leukocyte Cell Adhesion Molecule–mediated Homotypic Cell Adhesion through the Actin Cytoskeleton[V]

Judith M. D. T. Nelissen,* Inge M. Peters,† Bart G. de Grooth,† Yvette van Kooyk,* and Carl G. Figdor*‡

*Department of Tumor Immunology, University Medical Center, NL-6525 EX Nijmegen, The Netherlands; and †Department of Biophysical Techniques, University of Twente, NL-7500 AE Enschede, The Netherlands

Submitted January 27, 2000; Revised March 17, 2000; Accepted March 22, 2000
Monitoring Editor: Martin Schwartz

Restricted expression of activated leukocyte cell adhesion molecule (ALCAM) by hematopoietic cells suggests an important role in the immune system and hematopoiesis. To get insight into the mechanisms that control ALCAM-mediated adhesion we have investigated homotypic ALCAM–ALCAM interactions. Here, we demonstrate that the cytoskeleton regulates ALCAM-mediated cell adhesion because inhibition of actin polymerization by cytochalasin D (CytD) strongly induces homotypic ALCAM–ALCAM interactions. This induction of cell adhesion is likely due to clustering of ALCAM at the cell surface, which is observed after CytD treatment. Single-particle tracking demonstrated that the lateral mobility of ALCAM in the cell membrane is increased 30-fold after CytD treatment. In contrast, both surface distribution and adhesion of a glycosylphosphatidylinositol (GPI)-anchored ALCAM mutant are insensitive to CytD, despite the increase in lateral mobility of GPI-ALCAM upon CytD treatment. This demonstrates that clustering of ALCAM is essential for cell adhesion, whereas enhanced diffusion of ALCAM alone is not sufficient for cluster formation. In addition, upon ligand binding, both free diffusion and the freely dragged distance of wild-type ALCAM, but not of GPI-ALCAM, are reduced over time, suggesting strengthening of the cytoskeleton linkage. From these findings we conclude that activation of ALCAM-mediated adhesion is dynamically regulated through actin cytoskeleton-dependent clustering.

INTRODUCTION

Activated leukocyte cell adhesion molecule (ALCAM [CD166]) was first identified by Bowen *et al.* (1995) on activated leukocytes. Uchida *et al.* (1997) identified hematopoietic cell antigen, which is identical to ALCAM, on hematopoietic stem cells and myeloid progenitors. ALCAM is a member of the immunoglobulin (Ig) superfamily and consists of five extracellular Ig domains. It is a highly glycosylated type I transmembrane molecule with a short (32-aa) cytoplasmic tail and an observed molecular mass of 105 kDa. Besides expression on hematopoietic cells, ALCAM is widely expressed on nonhematopoietic cells such as metastasizing melanoma (Degen *et al.*, 1998), neuronal cells (Tanaka *et al.*, 1991), mesenchymal stem cells (Bruder *et al.*, 1998), bone marrow stromal cells (Cortes *et al.*, 1999), and hematopoiesis-supporting osteoblastic cells (Nelissen *et al.*, 2000).

ALCAM has a unique restricted expression pattern on hematopoietic cells. Although absent on resting peripheral blood lymphocytes, ALCAM becomes rapidly expressed upon polyclonal activation in vitro, reaching a maximum after 3 d of culture and decreasing to undetectable levels by day 8 (Bowen *et al.*, 1995). Similarly, monocytic cells in inflamed synovium from rheumatoid arthritis patients express much higher levels of ALCAM compared with resting monocytes (Levesque *et al.*, 1998). In addition, in vitro-generated monocyte-derived dendritic cells express high levels of ALCAM (J.M.D.T. Nelissen, unpublished results). These findings suggest a role in inflammation. Furthermore, a well-defined subpopulation of $CD34^+$ bone marrow cells expresses ALCAM (Uchida *et al.*, 1997), as well as the sur-

[V] Online version of this article contains video material for Figures 1–8. Online version available at 222.molbiolcell.org.

‡ Corresponding author. E-mail address: C.Figdor@mailbox.kun.nl.

Abbreviations used: ALCAM, activated leukocyte cell adhesion molecule; CLSM, confocal laser scan microscopy; CytD, cytochalasin D; ERM, ezrin–radixin–moesin; GPI, glycosylphosphatidylinositol; ICAM, intercellular adhesion molecule; Ig, immunoglobulin; K562-ALCAM, K562 cells transfected with ALCAM; K562-GPI-ALCAM, K562 cells transfected with GPI-anchored ALCAM; LatA, latrunculin A; RT, room temperature; SPT, single-particle tracking.

rounding bone marrow stromal cells (Cortes *et al.*, 1999), hinting at a role in hematopoiesis. Thus far, the function of ALCAM in the immune system and in hematopoiesis is unknown.

In addition to its ability to bind CD6, ALCAM mediates homotypic ALCAM–ALCAM interactions (Bowen *et al.*, 1995; Uchida *et al.*, 1997). Although ALCAM–CD6 interactions have been thoroughly studied (Skonier *et al.*, 1996; Aruffo *et al.*, 1997; Bowen and Aruffo, 1999), the mechanism underlying homotypic ALCAM–ALCAM adhesion remains largely elusive.

Ligation of integrins, cadherins, selectins, and Ig superfamily adhesion molecules results in signal transduction over the membrane into the cell (for a recent review, see Aplin *et al.*, 1998). These outside-in signals are generated either by the adhesion receptor itself or by associated molecules. To date, it is unclear whether ligation of ALCAM results in intracellular signaling. Integrins and an increasing number of other surface proteins are associated with and regulated by cytoskeletal components (Dubreuil *et al.*, 1996; Lub *et al.*, 1997; Balzar *et al.*, 1998; Suter *et al.*, 1998; Evans *et al.*, 1999). Ligation of the conformation-sensitive integrin adhesion receptors often results in cytoskeleton-dependent clustering of molecules and morphological changes that affect the adhesive behavior of cells. A well-documented example in which the dynamic regulation of cell–cell contacts is essential is the formation of the immunological synapse, or supramolecular activation complex, during T cell activation. The formation of this complex is orchestrated by a series of interactions and recruitment of costimulatory and adhesion molecules and depends strongly on cytoskeletal reorganization (Monks *et al.*, 1998; Wulfing and Davis, 1998; Grakoui *et al.*, 1999).

These observations and the diversity of cellular processes in which ALCAM is involved led us to hypothesize that ALCAM-mediated homotypic adhesion is tightly regulated. By analyzing the membrane distribution and the lateral mobility of ALCAM in the cell membrane, we now demonstrate that the actin cytoskeleton dynamically regulates ALCAM-mediated homotypic cell adhesion.

MATERIALS AND METHODS

Chemicals and Antibodies

All chemicals were purchased from Sigma (Zwijndrecht, The Netherlands) unless stated otherwise. Stock solutions of cytochalasin D (CytD) and latrunculin A (LatA) were prepared in DMSO and stored at −20°C. Anti-ALCAM monoclonal antibodies J4-81 (IgG1 isotype) and FITC-conjugated J4-81 were purchased from Antigenix America (Franklin Square, NY). AZN-L50 (IgG2A isotype) was generated in our laboratory by immunizing BALB/c mice with K562 cells transfected with ALCAM (K562-ALCAM). Goat anti-human Fc-$(Fab')_2$ fragments were purchased from Jackson ImmunoResearch (West Grove, PA), and FITC-conjugated goat anti-mouse $(Fab')_2$ fragments were obtained from Zymed (San Francisco, CA). FITC-conjugated goat anti-human Fc-$(Fab')_2$ fragments were purchased from Cappel (West Chester, PA).

Cells, Cultures, and Expression Constructs

All media, sera, and antibiotics were purchased from Life Technologies (Breda, The Netherlands). All culture media were supplemented with 1% antibiotics and antimycotics. Myelomonocytic KG1 cells were cultured in Iscove's modified Dulbecco's medium containing 10% FCS. Erythroleukemic K562 cells were cultured in RPMI 1640 medium containing 10% FCS.

For stable transfection of K562, the full-length ALCAM cDNA (obtained from Dr. G. Swart, Department of Biochemistry, University Medical Center, Nijmegen, The Netherlands) was cloned into pRc/CMV (containing a neomycin resistance gene; Invitrogen, San Diego, CA). K562 cells were transfected by electroporation with a Gene Pulser (Bio-Rad, Hercules, CA) at 960 μF and 230 V, resulting in K562-ALCAM. Glycosylphosphatidylinositol (GPI)-anchored ALCAM was constructed by cloning the extracellular domains of ALCAM into pSG-DAF (a pSG8-based expression vector encoding the GPI-anchoring motif from decay accelerating factor; provided by Dr. G. ten Dam, Department of Cell Biology, University Medical Center) by PCR. The resulting ALCAM-DAF construct was recloned into pRc/CMV. K562 was transfected with this expression construct to generate K562 cells transfected with GPI-anchored ALCAM (K562-GPI-ALCAM). After stable transfection, K562 cells were maintained in a 3:1 mixture of RPMI 1640 medium containing 10% FCS and Iscove's modified Dulbecco's medium containing 5% FCS and selected with 2 mg/ml G418. After staining with FITC-conjugated ALCAM antibody J4-81, transfected cells were sorted at least three times with a Coulter Epics Elite cell sorter (Coulter Electronics, Hialeah, FL) to obtain a homogeneous population of cells.

For generation of chimeric ALCAM-Fc constructs, the five extracellular domains of ALCAM were cloned by PCR into pIg1 (obtained from Dr. D. Simmons, Medical Research Council, London, United Kingdom) to generate pALCAM-Ig. pALCAM-Ig was cotransfected with pEE14 (provided by Dr. M. Robinson, Celltech, Berkshire, United Kingdom) in Chinese hamster ovary-K1 cells by calcium phosphate transfection and selected on glutamine free RPMI 1640 medium containing 10% dialyzed FCS and 50 μM L-methionine sulphoximine. ALCAM-Fc fusion protein was purified from culture supernatant by protein G affinity chromatography (Amersham Pharmacia Biotech, Uppsala, Sweden). The concentration of purified ALCAM-Fc was determined with a human Fc-specific ELISA using human IgG1 as a standard.

Flow Cytometry

Cells were washed with PBA (PBS containing 1% BSA and 0.05% NaN_3) and stained for 30 min at 4°C with primary antibody (2–5 μg/ml in PBA). Cells were washed with PBA and incubated with FITC-conjugated goat anti-mouse $(Fab')_2$ secondary antibody. After washing, cells were analyzed on a FACScan analyzer (Becton Dickinson, Oxnard, CA). The gates were set to exclude dead cells, and 5000 gated cells were analyzed. Data are displayed as histograms of fluorescence intensity versus cell count.

Plate Adhesion Experiments

Flat-bottom Maxisorp 96-well plates (Nunc, Roskilde, Denmark) were coated with 4 μg/ml goat anti-human-Fc-$(Fab')_2$ in TSM (20 mM Tris, 150 mM NaCl, 1 mM $CaCl_2$, and mM $MgCl_2$, pH 8.0) for 1 h. The plates were blocked with 1% (wt/vol) BSA in TSM for 30 min and subsequently coated with 250 ng/ml ALCAM-Fc (or concentrations as stated in text) in TSM and 1% BSA for 1 h. All incubations were carried out at 37°C. Cells (20,000 per well) were labeled with Calcein-AM (Molecular Probes, Eugene, OR) in PBS for 30 min at 37°C and washed with PBS. CytD (2.5 μg/ml unless noted otherwise), LatA (Molecular Probes, 5 μg/ml), nocodazole (5 μg/ml), acrylamide (4 mM), sodium azide (10 mM), and deoxyglucose (50 mM) pretreatment was given by incubation of the cells for 30 min at 37°C in medium. Antibody AZN-L50 (10 μg/ml) was preincubated for 5–10 min at room temperature (RT). Cells were allowed to adhere in triplicate wells to the coated plates for 45 min in culture medium at 37°C in the presence or absence of the indicated mAb. Nonadherent cells were removed by repeated washing with TSM and 0.5% BSA at 37°C. Cells were lysed with lysis buffer (50

mM Tris and 0.1% SDS), and fluorescence was quantified in a cytofluorometer (PerSeptive Biosystems, Foster City, CA). Adhesion was expressed as the mean percentage ± SD of bound cells from triplicate wells. ALCAM-specific adhesion is calculated by subtracting the adhesion in the presence of both blocking antibody and stimulus from the adhesion in the presence of the stimulus alone.

Confocal Laser Scan Microscopy (CLSM)

Where indicated, cells were treated with CytD (2.5 μg/ml) for 20 min at 37°C. Cells were fixed with 1% paraformaldehyde and stained for 30 min at RT with the mAb AZN-L50 and subsequently incubated with FITC-conjugated goat anti-mouse $(Fab')_2$ fragments for 30 min at RT. Cells were mounted on poly-L-lysine–coated glass slides, and cell surface distribution was analyzed by CLSM at 488 nm with a krypton–argon laser on an MRC1000 confocal microscope (Bio-Rad). The instrument settings were gain, 1500; iris, 0.7 μm; laser, 30%; lens, 60×; and magnification, 2×.

Single-Particle Tracking (SPT) and Dragging Measurements

Ligand-coated, carboxylated polystyrene beads (0.918 μm; Polysciences, Eppelheim, Germany) were prepared essentially as described previously (Geijtenbeek *et al.*, 1999). In brief, streptavidin is covalently coupled to the beads, followed by an incubation with biotinylated goat anti-human $Fc(Fab')_2$ fragments. Next, 1 ng of ALCAM-Fc in 0.5 ml was added to obtain $ALCAM^{lo}$ beads, or 250 ng were added to obtain saturated beads ($ALCAM^{hi}$ beads) as determined by flow cytometry using calibration beads (Quantum 24; Flow Cytometry Standards, San Juan, Puerto Rico) as a standard. $ALCAM^{lo}$ beads contain ~80 molecules per bead, allowing only one or few interactions. Taking into account the dimensions of the beads and the cells, it is estimated that at most 10% of the bead will be in contact with the cell; the maximum number of molecular interactions is 8. $ALCAM^{hi}$ beads contain ~2000 molecules per bead, enabling multiple interactions.

The day before the experiment the cells were prepared at 5×10^5 cells/ml. For a number of experiments the cells were pretreated with 2.5 μg/ml CytD or with its solvent, DMSO (0.25%), at 37°C for 30 min. The cells were attached to poly-L-lysine–coated cover glasses.

The SPT and dragging experiments were carried out at RT. A detailed description of the method and experimental setup is given elsewhere (Peters *et al.*, 1998, 1999). Briefly, a polystyrene bead coated with ALCAM molecules was allowed to bind to the cell for 5 s using optical tweezers. After checking whether this bead was bound to the cell, an SPT or dragging measurement was performed. The two-dimensional motion of the receptors in the cell membrane was measured during 120 s with a sampling frequency of 100 Hz and nanometer resolution using a focused HeNe laser. The bead was positioned in the center of the beam close to the focus. Displacement of the bead from the center of the beam causes a deflection of the beam that is measured by a position-sensitive detector. To avoid forces acting on the bead and consequently on the receptors, a feedback system was implemented that maintained the bead in the center of the laser beam throughout the measurements by displacing the sample cell with respect to the laser beam.

To investigate whether the receptors could be dragged over the cell membrane using small forces (<5 pN), a similar optical tweezers setup with a diode laser was used (Peters *et al.*, 1999). The optical trap (with a trap stiffness of ~8 pN/μm) was moved over the cell surface at a speed of 200 nm/s. The direction of dragging was chosen randomly. The position of the bead was determined from the position of the trap and the position of the bead in the optical trap with nanometer resolution (Sako *et al.*, 1998).

RESULTS

Homotypic ALCAM–ALCAM Interactions Are Regulated by the Actin Cytoskeleton

To study ALCAM-mediated adhesion in detail, K562 cells were transfected with the full-length wild-type ALCAM cDNA to generate stable K562-ALCAM transfectants. The expression level of ALCAM on K562-ALCAM was comparable with that of the myelomonocytic cell line KG1, naturally expressing ALCAM (Figure 1A). Both cell lines readily bind soluble ALCAM with identical kinetics and affinity, indicating that ALCAM is functional in K562-ALCAM cells (J.M.D.T. Nelissen, unpublished results).

To investigate whether the cytoskeletal network regulates ALCAM-mediated adhesion, we tested the effect of a number of cytoskeleton inhibitors on ALCAM-mediated adhesion. We observed that, without any stimulus, ALCAM-expressing cells do not adhere to immobilized ALCAM-Fc. Interestingly, rather than inhibiting adhesion, the actin cytoskeleton inhibitors CytD and LatA significantly enhance adhesion (Figure 1B). CytD- and LatA-induced adhesion is ALCAM specific because the blocking ALCAM antibody AZN-L50 (J.M.D.T. Nelissen, unpublished results) inhibits both CytD- and LatA-induced adhesion. Similar results were obtained with KG1 cells. In contrast, treatment with nocodazole or acrylamide did not stimulate cell adhesion (Figure 1B), demonstrating that microtubuli and intermediary filaments are not involved the regulation of ALCAM-mediated adhesion.

Cytochalasin D-induced ALCAM-mediated Adhesion Is Concentration, Energy, and Temperature Dependent

To study the mechanism of CytD-induced ALCAM adhesion in more detail, we analyzed the dependence of adhesion on both the concentration of immobilized ALCAM-Fc and the concentration of CytD (Figure 2, A and B). CytD-induced cell adhesion is maximal when 250 ng/ml ALCAM-Fc is coated (Figure 2A) and at a concentration of 1.25 μg/ml CytD (Figure 2B), and CytD induced ALCAM-mediated cell adhesion is efficiently blocked with mAb AZN-L50 (Figure 2, A and B).

When cells are depleted from energy by a combination of sodium azide and deoxyglucose, CytD is not capable of stimulating adhesion (Figure 2C), showing that the CytD-induced adhesion is an active process. This notion is also supported by the finding that induction of ALCAM-mediated adhesion by CytD proved to be temperature sensitive. After preincubation with CytD at 37°C, cells do not adhere to immobilized ALCAM-Fc when incubated at room temperature or at 4°C (Figure 2D). Similarly, we observed that ALCAM-expressing KG1 cells can be stimulated by CytD to adhere to ALCAM-Fc–coated plates in an energy- and temperature-dependent manner. Together, these data strongly suggest that ALCAM-mediated adhesion is actively regulated by the actin cytoskeleton.

Cytochalasin D Alters the ALCAM Distribution at the Cell Surface

We hypothesized that the induction of adhesion by CytD is caused by clustering of ALCAM molecules at the cell sur-

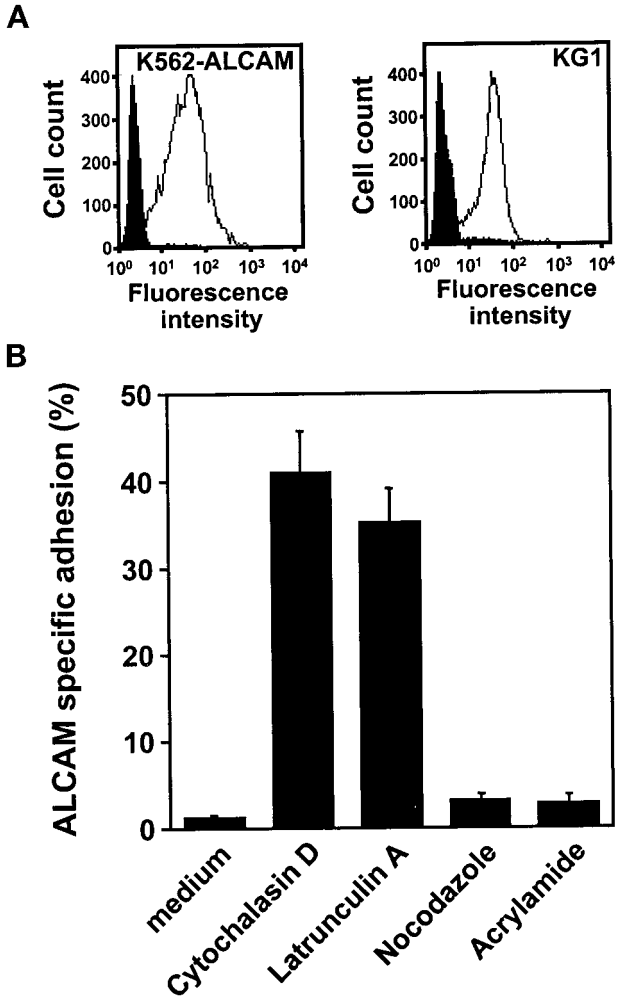

Figure 1. (A) Expression of ALCAM on K562-ALCAM and KG1. Shaded histograms represent the isotype-matched control, and open histograms represent expression of ALCAM, detected with mAb J4-81. (B) ALCAM-mediated adhesion is regulated by the actin cytoskeleton. K562-ALCAM cells were preincubated for 30 min at 37°C with or without cytochalasin D (2.5 μg/ml), latrunculin A (5 μg/ml), nocodazole (5 μg/ml), or acrylamide (4 mM) and subsequently allowed to adhere to an ALCAM-Fc–coated plate (250 ng/ml ALCAM-Fc) for 45 min at 37°C in the presence or absence of the ALCAM-blocking mAb AZN-L50. Specific adhesion is expressed as the mean percentage ± SD of adherent cells from triplicate wells after subtraction of the adhesion in the presence of the blocking mAb AZN-L50. Data are representative of three experiments.

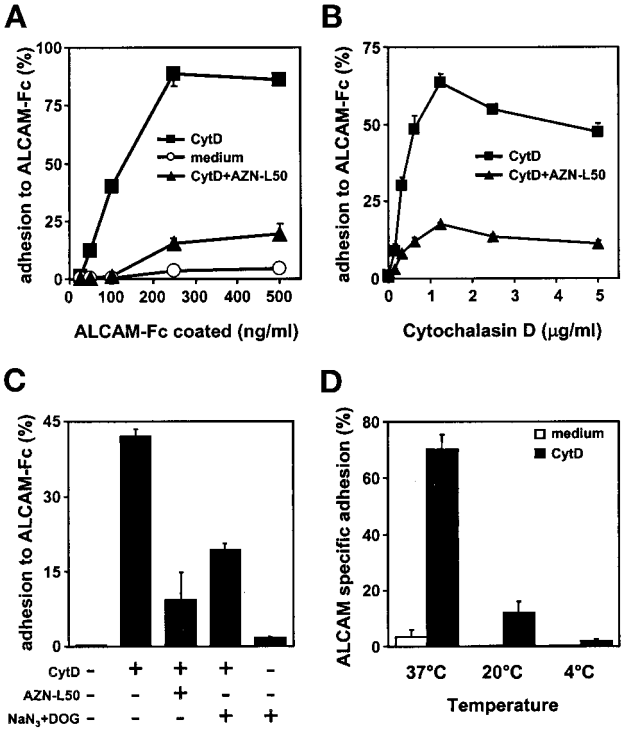

Figure 2. (A) CytD-induced adhesion is dependent on the concentration of ALCAM-Fc. Untreated (open circles) or CytD-pretreated (2.5 μg/ml, 30 min at 37°C; open squares) K562-ALCAM cells were allowed to adhere for 45 min at 37°C to increasing amounts of ALCAM-Fc. Addition of the blocking antibody AZN-L50 (closed triangles) inhibits CytD-induced adhesion. Adhesion was quantified, and the mean percentage of cells bound to the plate ± SD is depicted. One experiment of three is shown. (B) Induction of ALCAM-mediated adhesion is dependent on the concentration of CytD. K562-ALCAM cells were preincubated with increasing concentrations of CytD, and adhesion to an ALCAM-Fc–coated plate (250 ng/ml) in the absence (closed squares) or presence (closed triangles) of the blocking mAb AZN-L50 was determined. The mean percentage of cells ± SD bound to the plate is expressed. One representative experiment of three is shown. (C) Cytochalasin D-induced ALCAM adhesion is energy dependent. K562-ALCAM cells were preincubated with CytD (2.5 μg/ml) in the presence or absence of a combination of deoxyglucose (DOG, 50 mM) and sodium azide (NaN_3, 10 mM) to deprive the cells from energy or in the presence of the blocking mAb AZN-L50 (10 μg/ml). Control cells were preincubated with the combination of NaN_3 and DOG without CytD. Subsequently, adhesion to immobilized ALCAM-Fc (250 ng/ml) for 45 min at 37°C was determined. Adhesion is expressed as the mean percentage of cells bound to the plate from triplicate wells ± SD. Data are representative of three experiments. (D) CytD-induced ALCAM-mediated adhesion is temperature dependent. K562-ALCAM cells were preincubated with CytD (2.5 μg/ml, 37°C; black bars) and subsequently allowed to adhere for 45 min at 37°C, RT, or at 4°C. Specific adhesion is expressed as the mean percentage ± SD of adherent cells from triplicate wells after subtraction of the adhesion in the presence of the blocking mAb AZN-L50. One experiment of three is shown.

face, similar to what has been reported for integrins (Lub *et al.*, 1997; Yauch *et al.*, 1997). The enhanced avidity by clustering of ALCAM molecules at the cell surface might facilitate cell adhesion. When analyzing the membrane distribution of ALCAM by CLSM, we indeed observed that ALCAM is markedly clustered at the cell surface of CytD-treated K562-ALCAM cells (Figure 3B) compared with untreated controls (Figure 3A). In particular at cell–cell contact sites, ALCAM clustering is clearly seen, this despite the fact that the overall surface expression of ALCAM is not altered (Figure 3, C and D), excluding the possibility that CytD-induced adhesion is caused by de novo expression of

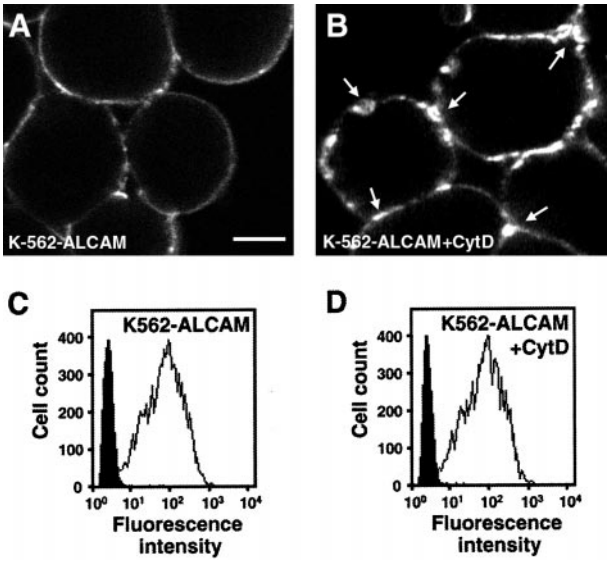

Figure 3. Analysis of the membrane distribution of ALCAM by CLSM. K562-ALCAM cells were pretreated without (A) or with CytD (2.5 μg/ml; B) and stained with mAb AZN-L50. For each preparation, similar instrument settings were used. Bar, 5 μm. Arrows indicate ALCAM clusters at the cell surface. Flow cytometric analysis of ALCAM expression as measured on K562-ALCAM before (C) and after (D) CytD treatment was performed on the same cell samples as used for CLSM and revealed that the overall cell surface expression of ALCAM remained unaltered.

ALCAM. Patches of high concentrations of ALCAM molecules likely account for the enhanced adhesion to the ALCAM-Fc–coated plate.

Cytochalasin D Increases the Lateral Mobility of ALCAM Molecules in the Cell Membrane

To prove the association of ALCAM with the actin cytoskeleton and to understand the mechanism of cluster formation at the cell surface, we performed SPT experiments, using an optical trap that allows tracking with nanometer resolution and high-frequency sampling, as previously described (Peters *et al.*, 1998). First, we used calibrated beads coated with minimal amounts of ALCAM-Fc (ALCAM^{lo} beads), allowing only one or very few molecular interactions. Two typical trajectories of single ALCAM molecules bound to ALCAM^{lo} beads attached to single ALCAM molecules on the cell surface of K562-ALCAM are shown (Figure 4A). The lateral mobility of single ALCAM molecules in the membrane is significantly increased after treatment of the cells with CytD (Figure 4B), demonstrating that the actin cytoskeleton restrains ALCAM-mediated lateral mobility. The slow (macro) and fast (micro) diffusion coefficients were calculated from the mean square displacement versus time interval plots as described (Peters *et al.*, 1999) and are plotted in Figure 4C. The mean slow diffusion coefficient increases 30-fold from $2.8 \times 10^{-12} \pm 5.6 \times 10^{-13}$ to $9.3 \times 10^{-11} \pm 5.3 \times 10^{-11}$ cm^2/s after CytD treatment (Table 1). Clearly, despite the formation of ALCAM clusters upon CytD treatment (as observed by CLSM analysis), ALCAM proteins diffuse much faster in the membrane of CytD-treated cells when compared with ALCAM molecules in untreated cells. We can exclude that the solvent DMSO (0.25%) causes this effect, because no significant changes is the lateral mobility are observed when the K562-ALCAM cells are treated with DMSO alone (Table 1).

The specificity of the interaction of the ALCAM-coated beads with the ALCAM-expressing cells was determined using intercellular adhesion molecule-1 (ICAM-1) Fc-coated beads as a control. Almost 60% of the ALCAM^{lo} beads bound to K562-ALCAM (34 of 58 beads). Only 11% of the ALCAM^{lo} beads bound to untransfected K562 cells (4 of 35). ICAM-1 Fc-coated beads showed background binding of 5% (2 of 40 beads). Thus, the interaction between ALCAM^{lo} beads and K562-ALCAM is specific.

Clear differences were observed when beads were coated with saturating amounts of ALCAM-Fc (ALCAM^{hi} beads), enabling the tracking of multiple ALCAM molecules bound to one bead. All ALCAM^{hi} beads bound to the cell within 3 s (15 of 15). Note that the lateral mobility of a group of ALCAM molecules bound to an ALCAM^{hi} bead is severely limited, and in some cases, movement of the bound molecules appears to be directional instead of random (Figure 4, D and F). Interestingly, despite this clearly restricted mobility in untreated cells, CytD treatment still dramatically increased the lateral mobility of ALCAM^{hi} beads (Figure 4, E and F). In addition, the diffusion coefficients of ALCAM^{hi} beads are virtually identical to the diffusion coefficients of ALCAM^{lo} beads in CytD-treated cells (Figure 4, C and F, and Table 1). These results demonstrate that ALCAM is indeed associated with the actin cytoskeleton, because dissociation from the actin cytoskeleton by CytD significantly enhances ALCAM mobility.

GPI-anchored ALCAM Adhesion and Membrane Distribution Is Not Regulated by the Actin Cytoskeleton

To prove that anchoring to the actin cytoskeleton is important for the regulation of ALCAM-mediated adhesion, we constructed a GPI-linked mutant of ALCAM in which both the cytoplasmic tail and the transmembrane region of ALCAM are replaced by a GPI anchor. We hypothesized that, because this mutant cannot directly bind to actin, adhesion and lateral mobility will be independent from the actin cytoskeleton. K562 cells stably transfected with GPI-anchored ALCAM were selected by flow cytometry to obtain K562-GPI-ALCAM cells that express GPI-anchored ALCAM at levels similar to those of wild-type K562-ALCAM (Figure 5A). GPI-ALCAM expressed by those cells is functional because it binds soluble ligand at least equally well as wild-type K562-ALCAM (our unpublished results).

As expected, we observed that neither CytD nor LatA can induce adhesion of K562-GPI-ALCAM to immobilized ALCAM-Fc (Figure 5B). These findings strongly support the notion that ALCAM-mediated adhesion is regulated by the actin cytoskeleton and is dependent on the presence of the cytoplasmic tail or transmembrane domain of ALCAM.

When K562-GPI-ALCAM cells are treated with CytD, the cell surface distribution remains unaltered (Figure 6, A and B), in contrast to wild-type ALCAM, which becomes clustered upon CytD treatment of the cells (Figure

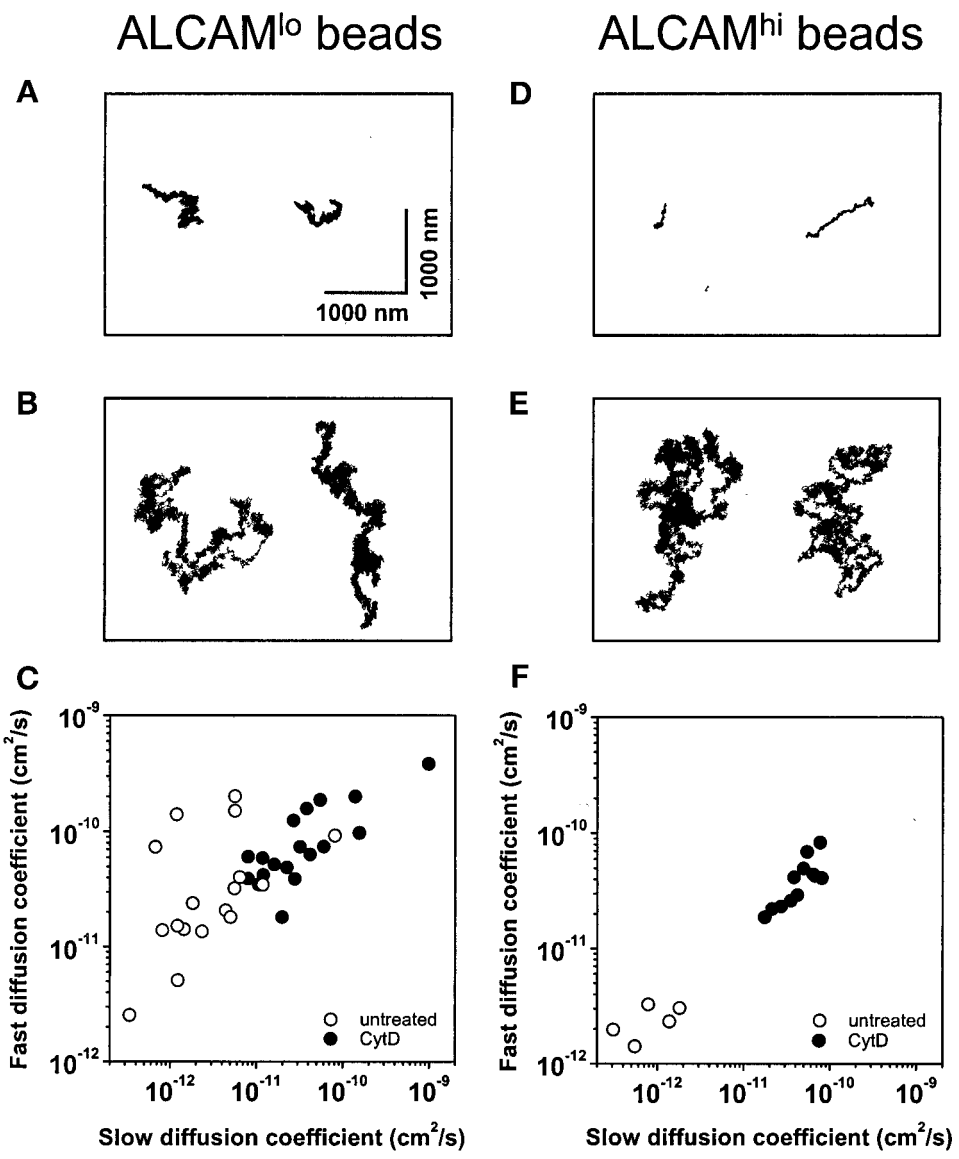

Figure 4. Lateral mobility of ALCAM molecules in the cell membrane is increased upon CytD treatment. Representative two-dimensional trajectories of ALCAM molecules attached to ALCAM^{lo} beads (A and B) and ALCAM^{hi} beads (D and E) in the absence (A and D) or presence (B and E) of CytD (2.5 μg/ml) are shown. Bars for A, B, D, and E are indicated in A. Trajectories were recorded during 120 s at a sampling rate of 100 Hz. Slow and fast diffusion coefficients were calculated from the mean square displacement versus time interval plots and are shown in C and F. Open circles represent untreated cells, and closed circles represent CytD-treated cells. Diffusion coefficients of single ALCAM molecules (ALCAM^{lo} beads; C) and of multiple molecules (ALCAM^{hi} beads; F) are shown. The average slow diffusion coefficients are summarized in Table 1.

3B). Also the cell surface expression of GPI-ALCAM is not influenced by CytD treatment (Figure 6, C and D). These findings strongly indicate that clustering of ALCAM after partial release from the cytoskeleton by CytD governs ALCAM-mediated adhesion.

Cytochalasin D Also Increases the Lateral Mobility of GPI-anchored ALCAM

We observed that movement of single GPI-ALCAM molecules in the membrane attached to ALCAM^{lo} beads is lim-

Table 1. Average slow diffusion coefficients of ALCAM-coated beads bound to ALCAM in the cell membrane

	Beads	Untreated ($\times 10^{-12}$ cm^2/s)	CytD treated ($\times 10^{-12}$ cm^2/s)	DMSO treated ($\times 10^{-12}$ cm^2/s)
K562-ALCAM	ALCAM^{lo}	2.75 ± 0.56	93 ± 53	5 ± 1.4
	ALCAM^{hi}	0.97 ± 0.28	47.6 ± 6.1	ND
K562-GPI-ALCAM	ALCAM^{lo}	2.0 ± 0.48	120 ± 68.7	14 ± 5.1

The mean − SD of the slow diffusion coefficients ($\times 10^{-12}$ cm^2/s) is shown. ND, not determined.

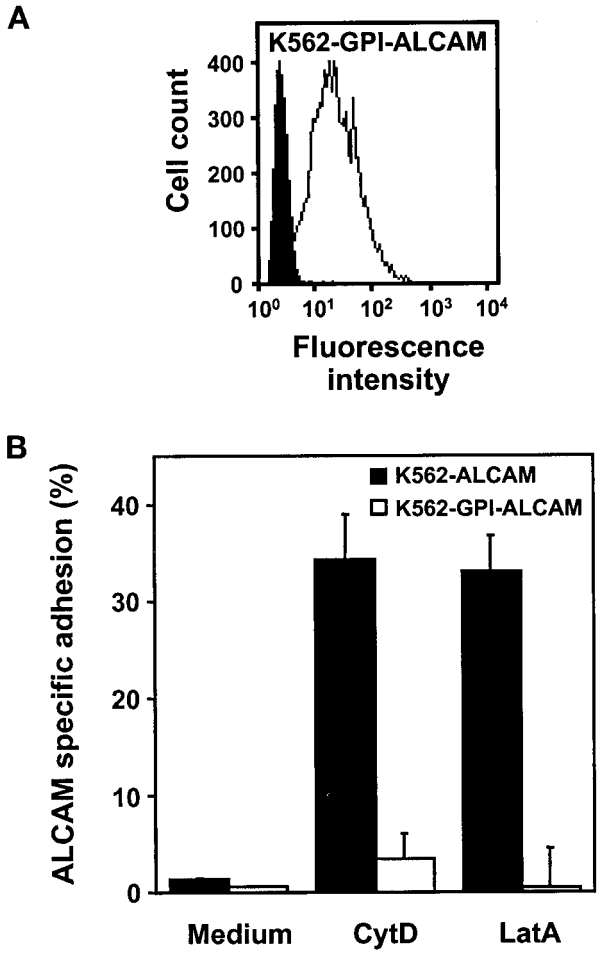

Figure 5. (A) Flow cytometric analysis of the surface expression of GPI-anchored ALCAM on K562-GPI-ALCAM using J4-81. The shaded histogram represents the isotype-matched control, and the open histogram represents J4-81 staining. Depicted is the fluorescence intensity versus the cell count. (B) GPI-anchored ALCAM-mediated adhesion cannot be induced by disruption of the actin cytoskeleton. K562-GPI-ALCAM cells (white bars) and K562-ALCAM cells (black bars), untreated or pretreated with CytD (2.5 μg/ml) or LatA (5 μg/ml), were allowed to adhere to immobilized ALCAM-Fc (250 ng/ml) for 45 min at 37°C, and ALCAM-specific adhesion was determined. Specific adhesion is expressed as the mean percentage ± SD of adherent cells from triplicate wells. Data are representative of four experiments.

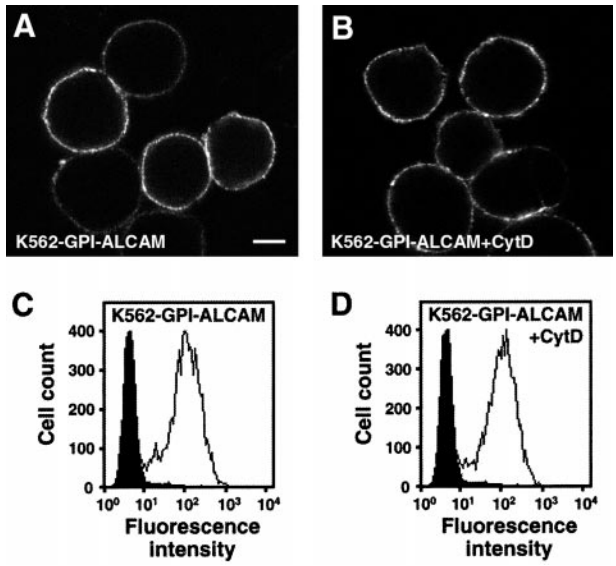

Figure 6. Analysis of the membrane distribution of GPI-anchored ALCAM by CLSM. K562-GPI-ALCAM cells were pretreated without (A) or with CytD (2.5 μg/ml; B) and stained with mAb AZN-L50. For each preparation, similar instrument settings were used. Bar, 5 μm. The cell surface distribution of GPI-ALCAM remains unaltered after CytD treatment. Flow cytometric analysis of ALCAM expression as measured on K562-GPI-ALCAM before (C) and after (D) CytD treatment was performed on the same cell samples as used for CLSM and revealed that ALCAM expression is not changed.

ited (Figure 7A), and diffusion coefficients of GPI-anchored molecules are remarkably similar to those of wild-type ALCAM molecules in the cell membrane (Figure 7C and Table 1). Surprisingly, we observed that the lateral mobility of GPI-ALCAM is also increased upon CytD treatment of the cells (Figure 7, A and B). The mean slow diffusion coefficients increase from $2.0 \times 10^{-12} \pm 4.8 \times 10^{-13}$ to $1.2 \times 10^{-10} \pm 6.9 \times 10^{-11}$ cm^2/s upon treatment of the cells with CytD. However, in contrast to wild-type ALCAM, in which DMSO did not affect the lateral mobility, we observed that addition of equivalent amounts of the solvent DMSO to the cells results in an intermediate increased lateral mobility of GPI-ALCAM (Figure 7D) with a mean slow diffusion coefficient of $1.4 \times 10^{-11} \pm 5.1 \times 10^{-12}$ (Table 1). Therefore, we cannot exclude that the increased lateral mobility of GPI-anchored ALCAM is caused by DMSO rather than by disrupting the actin cytoskeleton using CytD. From these findings we conclude that enhancing the lateral mobility of GPI-ALCAM per se, either by CytD or by DMSO, is not sufficient to form clusters at the cell surface, which is required to mediate stable cell adhesion.

Decrease of Diffusion and Inhibition of Dragging of Wild-Type ALCAM over Time

To investigate whether the cell responds to ALCAM^{lo} beads bound to ALCAM at the cell surface, we analyzed changes in mobility over time. We observed that free diffusion of wild-type ALCAM (Figure 8A) is markedly reduced 10 min after initial tracing (Figure 8B). In some cases, the mobility even became directional (Figure 8B). This decreased diffusion and increase in directional movement is not observed for CytD-treated cells or for GPI-ALCAM, indicating that inhibition is likely due to actin reorganization (Felsenfeld *et al.*, 1996; Choquet *et al.*, 1997).

Besides measuring free diffusion of molecules in the cell membrane, the optical trap allows dragging of bound beads over the cell surface. When dragging wild-type ALCAM by displacing the optical trap along the cell membrane with a speed of 200 nm/s at a trap force of ~8 pN/μm, we observed in untreated cells that molecules cannot move freely

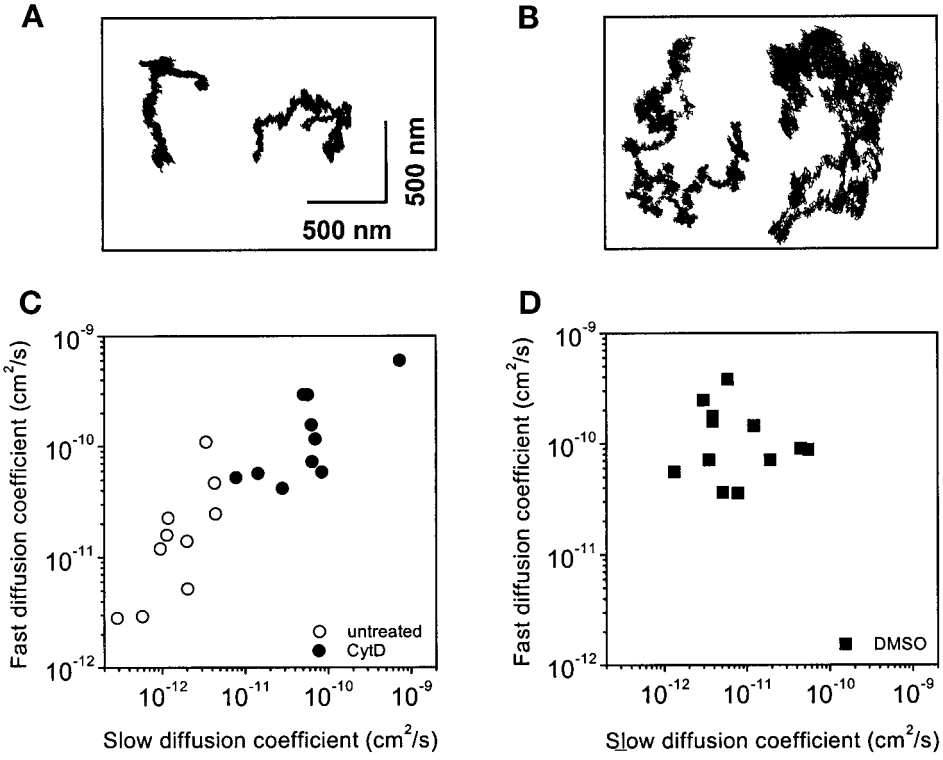

Figure 7. The lateral mobility of GPI-ALCAM molecules in the cell membrane is increased upon CytD treatment. (A and B) Two-dimensional trajectories of GPI-ALCAM molecules attached to ALCAM^{lo} beads in the absence (A) or presence (B) of CytD (2.5 μg/ml) are shown. Trajectories were recorded during 120s at a sampling rate of 100 Hz. Slow and fast diffusion coefficients of the GPI-anchored ALCAM molecules were calculated from the mean square displacement versus time interval plots and are shown in C. Open circles represent untreated cells, and closed circles represent CytD-treated cells. (D) Slow and fast diffusion coefficients of DMSO-treated (solvent, 0.25%) cells are plotted and are also increased. The average slow diffusion coefficients are summarized in Table 1.

(Figure 8C). Occasional "jumps" are observed and after 5–10 s, and the bead can no longer be displaced at this trap strength. Apparently, ALCAM molecules become firmly attached to the actin cytoskeleton within 10 s after ligation. When cells are pretreated with CytD, free movement of the beads over the cell surface is observed at all times (Figure 8D). For 6 of 12 measurements with wild-type ALCAM, we observed this reduced freely dragged distance of the molecules. For CytD-treated K562-ALCAM, six of seven beads could be moved freely (Table 2).

In contrast, GPI-anchored ALCAM can be freely moved over the cell membrane in both untreated (Figure 8E) and in CytD-treated cells (Figure 8F). The slight deviation of the bead from the position of the trap as seen in Figure 8, D and F, increases in time and is due to the drag force that is required to pull the molecule through the membrane, which results in a slight displacement of the bead from the center of the optical trap. Dragging the GPI-anchored molecules for extended periods resulted only once (one of seven) in reduced freely dragged distance of the molecules, whereas five beads could be pulled freely. At the membrane of CytD-treated K562-GPI-ALCAM, five of five beads could be freely moved (Table 2).

These results provide further evidence that ALCAM-mediated adhesion is regulated by an actin cytoskeleton-dependent mechanism, which will eventually lead to stabilization of ALCAM-mediated cell adhesion.

DISCUSSION

ALCAM is a novel member of the Ig superfamily of adhesion molecules. Besides binding to CD6, ALCAM mediates homotypic ALCAM–ALCAM interactions (Bowen *et al.*, 1995; Uchida *et al.*, 1997). Unraveling the mechanism that regulates ALCAM-mediated interactions will help in understanding the biological function of ALCAM in the immune system and in hematopoiesis. In this report we demonstrate that homotypic ALCAM-mediated cell adhesion is tightly regulated through the actin cytoskeleton by the formation of clusters of molecules at the cell surface.

We observed that ALCAM-mediated adhesion is induced when the actin cytoskeleton is chemically disrupted by low concentrations of CytD or by LatA. Similarly, low concentrations of CytD (0.1–3 μg/ml), which do not cause total disruption of the actin cytoskeleton (Kucik *et al.*, 1996), were previously shown to induce adhesion of β1 and β2 integrins as well (Kucik *et al.*, 1996; Lub *et al.*, 1997; Yauch *et al.*, 1997). Microscopic analysis of CytD-treated K562-ALCAM showed that this partial release of ALCAM from the actin cytoskeleton enables the formation of ALCAM clusters at the cell surface. These observations confirm the hypothesis of others, who have proposed that homotypic clustering of ALCAM molecules enhances the avidity of ALCAM (Bowen *et al.*, 1996; Aruffo *et al.*, 1997). Also, aggregation of recombinant ALCAM molecules has been described (Skonier *et al.*, 1996). Here we present experimental evidence that clustering of membrane-bound ALCAM is essential for stable cell adhesion.

Our observations are similar to those reported for integrins describing that upon CytD treatment of resting peripheral blood lymphocytes, both increased mobility and clustering of the $\alpha_L\beta_2$ integrin LFA-1 are observed, resulting in higher avidity for its ligand ICAM-1 (Kucik *et al.*, 1996; Lub *et al.*, 1997). Also, $\alpha_4\beta_1$ integrin adhesive activity is regulated

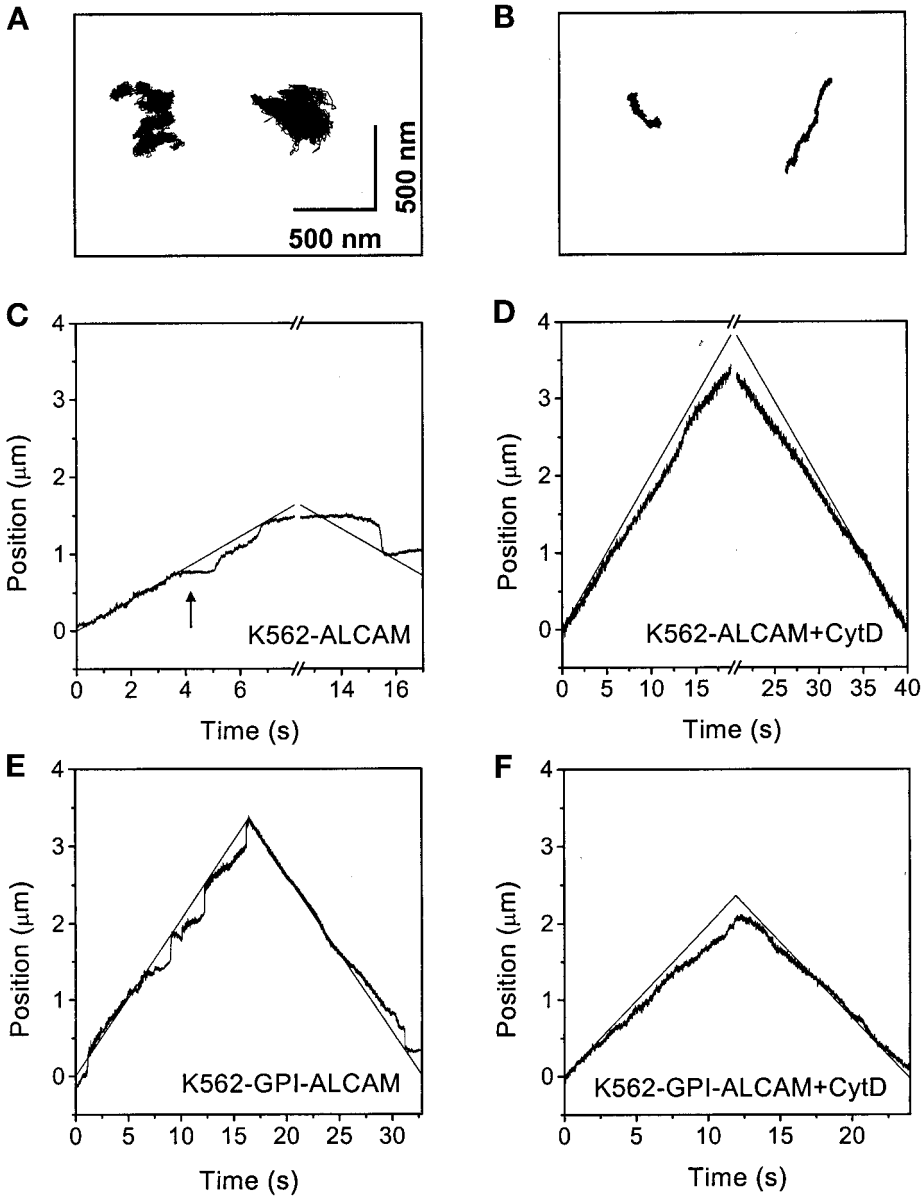

Figure 8. Mobility of ALCAM molecules is altered over time. (A and B) Initial two-dimensional free diffusion trajectories of wild-type ALCAM engaged by ALCAM^{lo} beads (A) and trajectories of corresponding beads 10 min after initial tracing (B). The position of the beads was recorded during 60 s at a sampling rate of 100 Hz. Over time, the free diffusion of ALCAM is decreased. (C–F) Force measurements of wild-type and GPI-ALCAM molecules. The optical trap was moved along the cell membrane at 200 nm/s. The position of the trap relative to the starting point (0 μm) is shown as a function of time by the thin line. The position relative to the starting point (0 μm) of the bead and, accordingly, the position of the ALCAM molecules in the membrane are shown as a function of time by the solid line. The positions were measured with a sampling frequency of 100 Hz. Wild-type ALCAM is analyzed in C and D in the absence (C) or presence (D) of CytD (2.5 μg/ml). GPI-ALCAM is analyzed in E and F in the absence (E) or presence (F) of CytD (2.5 μg/ml). In A, the molecule is relatively mobile but becomes more firmly attached already after 4 s (arrow), and firm attachment is most clearly seen in the reverse movement of the trap. CytD-treated wild-type ALCAM as well as CytD-treated or untreated GPI-ALCAM molecules are in all cases freely pulled over the membrane for extended periods with long freely dragged distances. The x-axis break in C and D represents the time that the bead was lost from the center of the trap, either because of restraint of the bead (C) or because of the fact that the trap reached the edges of the cell (D) before the trap was reversed.

through receptor diffusion and clustering (Yauch *et al.*, 1997). Actin cytoskeleton-driven clustering of adhesion receptors at the cell surface appears to be a general mechanism used by cells to dynamically regulate cell adhesion.

Pretreatment of K562-GPI-ALCAM with CytD does not lead to formation of GPI-ALCAM clusters at the cell surface. This finding suggests that at least partial association with cytoskeletal components through the cytoplasmic domain or transmembrane region, which are lacking the GPI-anchored mutant, provides the driving force for stabilization of clustering of ALCAM molecules at the cell membrane. Alternatively, parts of the cytoplasmic or transmembrane domains may be required to form clusters, either directly or via associated molecules. GPI-anchored molecules tend to be targeted to specialized microdomains (cholesterol-enriched lipid rafts) in the cell membrane (Cebecauer *et al.*, 1998; Varma and Mayor, 1998), and this may actively restrain GPI-anchored ALCAM from clustering. However, the ability to form ALCAM clusters at the cell surface is a prerequisite for stable ALCAM-mediated homotypic adhesion.

The observation that GPI-anchored ALCAM is not spontaneously active because of increased lateral diffusion further demonstrates the importance of linkage of ALCAM to the actin cytoskeleton. Replacement of the transmembrane and cytoplasmic domains for a GPI anchor does not significantly alter the lateral diffusion of ALCAM. This is in agreement with previous findings showing that the lateral mobility of transmembrane proteins is only marginally affected by the presence of a GPI anchor compared with a transmembrane domain (Zhang *et al.*, 1991; Simson *et al.*, 1998).

Table 2. Dragging properties of ALCAM molecules

Event	K562-ALCAM		K562-GPI-ALCAM	
	Untreated	CytD treated	Untreated	CytD treated
Immobile				
From start	4/12	0/7	1/7	0/5
Over time[a]	6/12	0/7	1/7	0/5
Freely moving	2/12	7/7	5/7	5/5

Beads were dragged through the cell membrane with a speed of 200 nm/s. The dragging properties of single ALCAM molecules are classified as immobile or freely moving.

[a] Immobile over time designates beads that display reduction in mobility within 10 s.

We used a dedicated SPT device that allows single-particle measurements with nanometer resolution and a high sampling frequency (100 Hz). Our measurements show that ALCAM molecules diffuse more freely over the plasma membrane in CytD-treated cells compared with untreated control cells for both ALCAM^{lo} and ALCAM^{hi} beads. Taking into account that wild-type ALCAM becomes clustered at the cell surface upon CytD treatment and that ALCAM^{hi} beads will engage more molecules in the membrane than ALCAM^{lo} beads, we can conclude that for ALCAM mobility the cluster size is not limiting. This is supported by the findings of Kucik *et al.* (1999), who demonstrated that the mobility of membrane protein aggregates is only weakly dependent on aggregate size.

Unexpectedly, we noted that the lateral mobility of GPI-anchored ALCAM, which lacks both the cytoplasmic and transmembrane domains, is still affected by CytD treatment of the cells. Possibly, GPI-ALCAM is in close contact with other transmembrane molecules, and disconnecting these neighboring molecules from the cytoskeleton by disrupting the cortical actin cytoskeleton may also provide more freedom to the GPI-anchored ALCAM molecules. However, despite this increased mobility, it does not lead to the formation of stable ALCAM clusters as shown by CLSM analysis. Furthermore, we observed that the diffusion coefficients of GPI-anchored ALCAM, but not of wild-type ALCAM, are also influenced by the presence of the solvent 0.25% DMSO. This is in agreement with the findings of Winckler *et al.* (1999), who have shown that 0.4% DMSO uncouples the membrane from the underlying membrane skeleton. As mentioned earlier, GPI-anchored molecules tend to be targeted to specialized lipid raft-like microdomains, and those domains are likely more sensitive to DMSO.

The average slow diffusion coefficient of ALCAM is 2.8×10^{-12} cm^2/s, whereas the average diffusion coefficient for CytD-treated ALCAM is 30-fold increased to 9.3×10^{-11} cm^2/s. This correlates well with the findings from Sako *et al.* (1998), who postulated that molecules with diffusion coefficients $<1.5 \times 10^{-11}$ may be associated with the cytoskeleton, whereas molecules with diffusion coefficients $>1.5 \times 10^{-11}$ are not.

In wild-type ALCAM-expressing cells, ALCAM^{lo} beads display a higher mobility than ALCAM^{hi} beads. These findings demonstrate that the restraints from the cytoskeleton are much stronger when multiple molecules are engaged (ALCAM^{hi} beads) than when only a single molecule is bound (ALCAM^{lo} beads). This notion is further substantiated by the finding that bound ALCAM^{hi} beads appear to move in a directional manner, which is likely due to F-actin filament rearrangements.

We observed that 50% of the beads bound to wild-type ALCAM molecules became less mobile within 10 s when dragged over the plasma membrane with optical tweezers. This finding indicates adhesion-induced strengthening by actin polymerization and was not observed in CytD-pretreated cells and was observed only once with K562-GPI-ALCAM. Ligand-induced strengthening of the linkage to the cytoskeleton requires actin polymerization. It is therefore not observed in CytD-treated cells, despite the induction of clustering of ALCAM in these cells, because CytD inhibits actin polymerization. Besides increased attachment upon stressing of the receptor, free diffusion is also reduced upon binding of ALCAM^{lo} beads to untreated cells. Also, in the absence of force applied with the optical trap, free diffusion becomes directional, as is seen with ALCAM^{hi} beads, again hinting at ligand-induced cytoskeletal rearrangements. A similar mechanism was described by Felsenfeld *et al.* (1996), who showed that β1 integrins show directed movement in response to ligand. Attachment to the moving cytoskeleton is a critical step in the regulation of organized receptor movement at the surface. Similarly, Choquet *et al.* (1997) have shown that cells respond to the restraining force of extracellular matrix integrin ligands by strengthening the cytoskeleton linkages.

Our SPT measurements clearly demonstrate that ALCAM is dynamically associated with the actin cytoskeleton. Because both wild-type and GPI-ALCAM display similar diffusion coefficients, it is apparent that increased lateral mobility alone is not sufficient to induce adhesion. Although the formation of ALCAM clusters at the membrane is not solely dependent on the diffusive behavior of the molecules, it is essential to obtain stable adhesion. Clustering is a temperature- and energy-dependent process, and adhesion-induced cytoskeleton rearrangements likely account for stabilization of ALCAM clusters, enabling firm adhesion.

The small GTPases are key players in the organization of the actin cytoskeleton (Hall, 1998; Mackay and Hall, 1998). Rho was shown to regulate endothelial cell receptor clustering, and association of these receptors with the actin cytoskeleton leads to stable monocyte adhesion (Wojciak-Stothard *et al.*, 1999). Interestingly, it was recently reported that besides disrupting the actin cytoskeleton, CytD also triggers activation of the small GTPase RhoA (Ren *et al.*, 1999). Therefore, it is tempting to speculate that members of the Rho family of small GTPases participate in this cytoskeleton-dependent regulation of ALCAM-mediated homotypic adhesion.

It is interesting to note that ALCAM coimmunoprecipitates with a 30- to 35-kDa protein (Pesando *et al.*, 1986). Although the nature of this protein is currently unknown, it may form a link between ALCAM and the actin cytoskeleton. Besides this protein, no other proteins have thus far been reported to associate with ALCAM. Although the cytoplasmic domain does not contain any known protein binding motifs, it does contain an unusually high number of positively charged residues (25% lysine, overall 50% posi-

tively charged residues). Potential candidates are the ezrin–radixin–moesin (ERM) family of proteins that link transmembrane molecules to the actin cytoskeleton by binding to positively charged amino acid clusters in the cytoplasmic domains of a number of associated proteins (Yonemura *et al.*, 1998). Moreover, ERM proteins are essential for actin polymerization in response to Rho and Rac activation (Mackay *et al.*, 1997), and it has been demonstrated that linkage of transmembrane molecules to the actin cytoskeleton through ERM proteins is a prerequisite for Rho and Rac to induce cytoskeletal changes (Hall, 1998). In addition, Rho GTPases regulate lymphocyte polarization of adhesion molecules and ERM proteins (del Pozo *et al.*, 1999). Together, the ERM proteins are potential candidates to mediate linkage between ALCAM and cytoskeletal components. Future research will provide evidence of whether the ERM proteins and the Rho family of small GTPases are indeed involved in inside-out signaling of ALCAM.

Recently, Tomita *et al.* (2000) have demonstrated that in epithelial prostate cancer cells, recruitment of both E-cadherin and ALCAM to areas of cell–cell contact is dependent on the presence of α-N-catenin. Although they provide no evidence for a direct interaction between α-catenin and ALCAM, their findings suggest that also in nonhematopoietic cells, ALCAM distribution is regulated in a cytoskeleton-dependent manner.

In conclusion, we have demonstrated that ALCAM-mediated homotypic adhesion is actively regulated through the actin cytoskeleton by the formation and stabilization of ALCAM clusters at the cell surface upon ligation of the receptor.

ACKNOWLEDGMENTS

We are grateful to Dr. G. Swart for providing the full-length ALCAM cDNA. We thank Dr. G. ten Dam for providing the vector pSG-DAF, Dr. D. Simmons for the pIg1 vector, and Dr. M. Robinson for the vector pEE14.

REFERENCES

Aplin, A.E., Howe, A., Alahari, S.K., and Juliano, R.L. (1998). Signal transduction and signal modulation by cell adhesion receptors: the role of integrins, cadherins, immunoglobulin-cell adhesion molecules, and selectins. Pharmacol. Rev. *50*, 197–263.

Aruffo, A., Bowen, M.A., Patel, D.D., Haynes, B.F., Starling, G.C., Gebe, J.A., and Bajorath, J. (1997). CD6-ligand interactions: a paradigm for SRCR domain function? Immunol. Today *18*, 498–504.

Balzar, M., Bakker, H.A., Briaire-de-Bruijn, I.H., Fleuren, G.J., Warnaar, S.O., and Litvinov, S.V. (1998). Cytoplasmic tail regulates the intercellular adhesion function of the epithelial cell adhesion molecule. Mol. Cell. Biol. *18*, 4833–4843.

Bowen, M.A., and Aruffo, A. (1999). Adhesion molecules, their receptors, and their regulation: analysis of CD6-activated leukocyte cell adhesion molecule (ALCAM/CD166) interactions. Transplant. Proc. *31*, 795–796.

Bowen, M.A., Bajorath, J., Siadak, A.W., Modrell, B., Malacko, A.R., Marquardt, H., Nadler, S.G., and Aruffo, A. (1996). The amino-terminal immunoglobulin-like domain of activated leukocyte cell adhesion molecule binds specifically to the membrane-proximal scavenger receptor cysteine-rich domain of CD6 with a 1:1 stoichiometry. J. Biol. Chem. *271*, 17390–17396.

Bowen, M.A., Patel, D.D., Li, X., Modrell, B., Malacko, A.R., Wang, W.C., Marquardt, H., Neubauer, M., Pesando, J.M., and Francke, U. (1995). Cloning, mapping, and characterization of activated leukocyte-cell adhesion molecule (ALCAM), a CD6 ligand. J. Exp. Med. *181*, 2213–2220.

Bruder, S.P., Ricalton, N.S., Boynton, R.E., Connolly, T.J., Jaiswal, N., Zaia, J., and Barry, F.P. (1998). Mesenchymal stem cell surface antigen SB-10 corresponds to activated leukocyte cell adhesion molecule and is involved in osteogenic differentiation. J. Bone Miner. Res. *13*, 655–663.

Cebecauer, M., Cerny, J., and Horejsi, V. (1998). Incorporation of leukocyte GPI-anchored proteins and protein tyrosine kinases into lipid-rich membrane domains of COS-7 cells. Biochem. Biophys. Res. Commun. *243*, 706–710.

Choquet, D., Felsenfeld, D.P., and Sheetz, M.P. (1997). Extracellular matrix rigidity causes strengthening of integrin-cytoskeleton linkages. Cell *88*, 39–48.

Cortes, F., Deschaseaux, F., Uchida, N., Labastie, M.C., Friera, A.M., He, D., Charbord, P., and Peault, B. (1999). HCA, an immunoglobulin-like adhesion molecule present on the earliest human hematopoietic precursor cells, is also expressed by stromal cells in blood-forming tissues. Blood *93*, 826–837.

Degen, W.G., van Kempen, L.C., Gijzen, E.G., van Groningen, J.J., van Kooyk, Y., Bloemers, H.P., and Swart, G.W. (1998). MEMD, a new cell adhesion molecule in metastasizing human melanoma cell lines, is identical to ALCAM (activated leukocyte cell adhesion molecule). Am. J. Pathol. *152*, 805–813.

del Pozo, M.A., Vicente-Manzanares, M., Tejedor, R., Serrador, J.M., and Sanchez-Madrid, F. (1999). Rho GTPases control migration and polarization of adhesion molecules and cytoskeletal ERM components in T lymphocytes. Eur. J. Immunol. *29*, 3609–3620.

Dubreuil, R.R., MacVicar, G., Dissanayake, S., Liu, C., Homer, D., and Hortsch, M. (1996). Neuroglian-mediated cell adhesion induces assembly of the membrane skeleton at cell contact sites. J. Cell Biol. *133*, 647–655.

Evans, S.S., Schleider, D.M., Bowman, L.A., Francis, M.L., Kansas, G.S., and Black, J.D. (1999). Dynamic association of L-selectin with the lymphocyte cytoskeletal matrix. J. Immunol. *162*, 3615–3624.

Felsenfeld, D.P., Choquet, D., and Sheetz, M.P. (1996). Ligand binding regulates the directed movement of beta 1 integrins on fibroblasts. Nature *383*, 438–440.

Geijtenbeek, T.B., van Kooyk, Y., van Vliet, S.J., Renes, M.H., Raymakers, R.A., and Figdor, C.G. (1999). High frequency of adhesion defects in B-lineage acute lymphoblastic leukemia. Blood *94*, 754–764.

Grakoui, A., Bromley, S.K., Sumen, C., Davis, M.M., Shaw, A.S., Allen, P.M., and Dustin, M.L. (1999). The immunological synapse: a molecular machine controlling T cell. Science *285*, 221–227.

Hall, A. (1998). Rho GTPases and the actin cytoskeleton. Science *279*, 509–514.

Kucik, D.F., Dustin, M.L., Miller, J.M., and Brown, E.J. (1996). Adhesion-activating phorbol ester increases the mobility of leukocyte integrin LFA-1 in cultured lymphocytes. J. Clin. Invest. *97*, 2139–2144.

Kucik, D.F., Elson, E.L., and Sheetz, M.P. (1999). Weak dependence of mobility of membrane protein aggregates on aggregate size supports a viscous model of retardation of diffusion. Biophys. J. *76*, 314–322.

Levesque, M.C., Heinly, C.S., Whichard, L.P., and Patel, D.D. (1998). Cytokine-regulated expression of activated leukocyte cell adhesion molecule (CD166) on monocyte-lineage cells and in rheumatoid arthritis synovium. Arthritis Rheum. *41*, 2221–2229.

Lub, M., van Kooyk, Y., van Vliet, S.J., and Figdor, C.G. (1997). Dual role of the actin cytoskeleton in regulating cell adhesion mediated by the integrin lymphocyte function-associated molecule-1. Mol. Biol. Cell *8*, 341–351.

Mackay, D.J., Esch, F., Furthmayr, H., and Hall, A. (1997). Rho- and rac-dependent assembly of focal adhesion complexes and actin filaments in permeabilized fibroblasts: an essential role for ezrin/radixin/moesin proteins. J. Cell Biol. *138*, 927–938.

Mackay, D.J., and Hall, A. (1998). Rho GTPases. J. Biol. Chem. *273*, 20685–20688.

Monks, C.R., Freiberg, B.A., Kupfer, H., Sciaky, N., and Kupfer, A. (1998). Three-dimensional segregation of supramolecular activation clusters in T cells. Nature *395*, 82–86.

Nelissen, J.M.D.T., Torensma, R., Pluijter, M., Adema, G.J., Raymakers, R.A.P., van Kooyk, Y., and Figdor, C.G. (2000). Molecular analysis of the hematopoiesis supporting osteoblastic cell line U2-OS. Exp. Hematol. *28*, 422–432.

Pesando, J.M., Hoffman, P., and Abed, M. (1986). Antibody-induced antigenic modulation is antigen dependent: characterization of 22 proteins on a malignant human B cell line. J. Immunol. *137*, 3689–3695.

Peters, I.M., de Grooth, B.G., Schins, J.M., Figdor, C.G., and Greve, J. (1998). Three dimensional single-particle tracking with nanometer resolution. Rev. Sci. Instrum. *69*, 2762–2766.

Peters, I.M., van Kooyk, Y., van Vliet, S.J., de Grooth, B.G., Figdor, C.G., and Greve, J. (1999). 3D single-particle tracking and optical trap measurements on adhesion proteins. Cytometry *36*, 189–194.

Ren, X.D., Kiosses, W.B., and Schwartz, M.A. (1999). Regulation of the small GTP-binding protein Rho by cell adhesion and the cytoskeleton. EMBO J. *18*, 578–585.

Sako, Y., Nagafuchi, A., Tsukita, S., Takeichi, M., and Kusumi, A. (1998). Cytoplasmic regulation of the movement of E-cadherin on the free cell surface as studied by optical tweezers and single particle tracking: corralling and tethering by the membrane skeleton. J. Cell Biol. *140*, 1227–1240.

Simson, R., Yang, B., Moore, S.E., Doherty, P., Walsh, F.S., and Jacobson, K.A. (1998). Structural mosaicism on the submicron scale in the plasma membrane. Biophys. J. *74*, 297–308.

Skonier, J.E., Bowen, M.A., Emswiler, J., Aruffo, A., and Bajorath, J. (1996). Mutational analysis of the CD6 binding site in activated leukocyte cell adhesion molecule. Biochemistry *35*, 14743–14748.

Suter, D.M., Errante, L.D., Belotserkovsky, V., and Forscher, P. (1998). The Ig superfamily cell adhesion molecule, apCAM, mediates growth cone steering by substrate-cytoskeletal coupling. J. Cell Biol. *141*, 227–240.

Tanaka, H., Matsui, T., Agata, A., Tomura, M., Kubota, I., McFarland, K.C., Kohr, B., Lee, A., Phillips, H.S., and Shelton, D.L. (1991). Molecular cloning and expression of a novel adhesion molecule, SC1. Neuron *7*, 535–545.

Tomita, K., van Bokhoven, A., Jansen, C.F., Bussemakers, M.J., and Schalken, J.A. (2000) Coordinate recruitment of E-cadherin and ALCAM to cell-cell contacts by alpha-catenin. Biochem. Biophys. Res. Commun. *267*, 870–874.

Uchida, N., *et al*. (1997). The characterization, molecular cloning, and expression of a novel hematopoietic cell antigen from CD34+ human bone marrow cells. Blood *89*, 2706–2716.

Varma, R., and Mayor, S. (1998). GPI-anchored proteins are organized in submicron domains at the cell surface. Nature *394*, 798–801.

Winckler, B., Forscher, P., and Mellman, I. (1999). A diffusion barrier maintains distribution of membrane proteins in polarized neurons. Nature *397*, 698–701.

Wojciak-Stothard, B., Williams, L., and Ridley, A.J. (1999). Monocyte adhesion and spreading on human endothelial cells is dependent on Rho-regulated receptor clustering. J. Cell Biol. *145*, 1293–1307.

Wulfing, C., and Davis, M.M. (1998). A receptor/cytoskeletal movement triggered by costimulation during T cell activation. Science *282*, 2266–2269.

Yauch, R.L., Felsenfeld, D.P., Kraeft, S.K., Chen, L.B., Sheetz, M.P., and Hemler, M.E. (1997). Mutational evidence for control of cell adhesion through integrin diffusion/clustering, independent of ligand binding. J. Exp. Med. *186*, 1347–1355.

Yonemura, S., Hirao, M., Doi, Y., Takahashi, N., Kondo, T., and Tsukita, S. (1998). Ezrin/radixin/moesin (ERM) proteins bind to a positively charged amino acid cluster in the juxta-membrane cytoplasmic domain of CD44, CD43, and ICAM-2. J. Cell Biol. *140*, 885–895.

Zhang, F., Crise, B., Su, B., Hou, Y., Rose, J.K., Bothwell, A., and Jacobson, K. (1991). Lateral diffusion of membrane-spanning and glycosylphosphatidylinositol-linked proteins: toward establishing rules governing the lateral mobility of membrane proteins. J. Cell Biol. *115*, 75–84.